Plant Physiology and Biochemistry 139 (2019) 513–520

Contents lists available at ScienceDirect

Plant Physiology and Biochemistry

journal homepage: www.elsevier.com/locate/plaphy

Research article

Hydraulic recovery from xylem embolism in excised branches of twelve woody species: Relationships with parenchyma cells and non-structural carbohydrates

Patrizia Trifilò[a,*], Natasa Kiorapostolou[b], Francesco Petruzzellis[c], Stefano Vitti[c,d], Giai Petit[b], Maria A. Lo Gullo[a], Andrea Nardini[c], Valentino Casolo[d]

[a] Dipartimento di Scienze Chimiche, Biologiche, Farmaceutiche ed Ambientali, Università di Messina, Viale Ferdinando Stagno d'Alcontres 31, 98166, Messina, Italy
[b] Dipartimento Territorio e Sistemi Agro-Forestali, Università di Padova, Viale dell'Università 16, 35020, Legnaro, PD, Italy
[c] Dipartimento di Scienze della Vita, Università di Trieste, Via L. Giorgieri 10, 34127, Trieste, Italy
[d] Dipartimento di Scienze AgroAlimentari, Ambientali e Animali, Università di Udine, Via delle Scienze 91, 33100, Udine, Italy

ARTICLE INFO

Keywords:
Hydraulic failure
Embolism repair
Non-structural carbohydrates
Parenchyma cells
P_{50}

ABSTRACT

Embolism repair ability has been documented in numerous species. Although the actual mechanism driving this phenomenon is still debated, experimental findings suggest that non-structural carbohydrates (*NSC*) stored in wood parenchyma would provide the osmotic forces to drive the refilling of embolized conduits.

We selected 12 broadleaved species differing in vulnerability to xylem embolism (P_{50}) and amount of wood parenchyma in order to check direct evidence about the possible link(s) between parenchyma cells abundance, *NSC* availability and species-specific capacity to reverse xylem embolism.

Branches were dehydrated until ~50% loss of hydraulic conductivity was recorded (*PLC* ~50%). Hydraulic recovery (*ΔPLC*) and *NSC* content was, then, assessed after 1h of rehydration.

Species showed a different ability to recover their hydraulic conductivity from *PLC* ~ 50%. Removing the bark in the species showing hydraulic recovery inhibited the embolism reversal. Strong correlations between the *ΔPLC* and: *a)* the amount of parenchyma cells (mainly driven by the pith area), *b)* the consumption of soluble *NSC* have been recorded.

Our results support the hypothesis that refilling of embolized vessels is mediated by the mobilization of soluble *NSC* and it is mainly recorded in species with a higher percentage of parenchyma cells that may be important in the hydraulic recovery mechanism as a source of carbohydrates and/or as a source of water.

1. Introduction

Terrestrial plants face the contrasting needs of maintaining a relatively stable water content, while losing large amounts of water vapour to the atmosphere when stomata are open to allow CO_2 diffusion into the leaf (Raschke, 1976). In vascular homoiohydric plants, this delicate balance is made possible by continuous absorption of water from the soil, that is then transported to the foliage through the xylem conduits while under negative pressure (Nardini et al., 2018; Venturas et al., 2017).

Intense or prolonged drought events pose a serious threat to the survival of plants, including crops and forest trees (Lesk et al., 2016). Drought and heat waves reduce soil water availability and increase atmospheric evaporative demand, putting plants at risk of desiccation. Under these conditions, timely stomatal closure is a fundamental mechanism allowing plants to maintain their hydration status and resist drought stress (Martin-StPaul et al., 2017). However, under prolonged drought, plants can continue to lose significant amounts of water via residual cuticular transpiration (Schuster et al., 2017), leading to progressive dehydration and decreasing xylem pressure.

When xylem pressure drops below the species-specific critical thresholds, an air-phase can be aspirated into water-filled xylem conduits through pit membrane pores, leading to gas-filled and non-conductive elements (Mayr et al., 2014; Tyree and Sperry, 1989). When this so-called xylem embolism process spreads to a significant number of conduits in the plant body, leading to high loss of plant hydraulic conductance, the residual water transport capacity cannot assure adequate hydration of tissues and the plant can eventually die by terminal

---

[*] Corresponding author.
E-mail address: ptrifilo@unime.it (P. Trifilò).

https://doi.org/10.1016/j.plaphy.2019.04.013
Received 8 March 2019; Received in revised form 10 April 2019; Accepted 10 April 2019

desiccation (Choat et al., 2018; Nardini et al., 2013; Tyree et al., 2002). This typically occurs when xylem hydraulic conductance is reduced by more than 80% in angiosperm species (Nardini et al., 2013; Urli et al., 2013). However, even when trees experiencing non-lethal drought, they can also undergo xylem embolism and suffer from reduced hydraulic efficiency, which potentially translates in decreased photosynthesis, reduced content of non-structural carbohydrates (*NSC*) and progressive decline of tree vigour and health due to carbon starvation (Peguero-Pina et al., 2018; Tomasella et al., 2019; Zhang et al., 2015).

Although trees can recover full hydraulic functionality by producing new xylem conduits (Zhang et al., 2019), different studies have reported that some plants, under specific conditions, can refill embolized conduits with water (Beikircher and Mayr, 2017; Gleason et al., 2017; Love and Sperry, 2018; Savi et al., 2016; Trifilò et al., 2015; Yoshimura et al., 2016). Considering the importance of hydraulic recovery for the overall performance of forest trees and crops under future climate scenarios (Klein et al., 2018), and despite scepticism around the actual occurrence of this phenomenon *in planta* (Cochard and Delzon, 2013; Wheeler et al., 2013), the possible mechanisms allowing plants to refill embolized conduits have been subjected to intense scrutiny by several studies in recent years (Brodersen et al., 2018; Martorell et al., 2014; Nardini et al., 2018; Ooeda et al., 2017; Secchi and Zwieniecki, 2016; Trifilò et al., 2017). It has been shown that xylem embolism reversal is frequently accompanied by starch degradation and release of sugars in the conduits (Beikircher and Mayr, 2017; Salleo et al., 2009; Secchi and Zwieniecki, 2011, 2012; Tomasella et al., 2017; Yoshimura et al., 2016; Wang et al., 2018), apparently 'priming' the xylem for refilling via an osmotic mechanism when plants are rehydrated and xylem tension is released (Brodersen and McElrone, 2013; Knipfer et al., 2016; Nardini et al., 2011). In accordance, enhanced expression of several genes involved in *NSC* metabolism and transport, as well as of aquaporins have been reported in plants undergoing hydraulic recovery (Chitarra et al., 2014; Perrone et al., 2012; Secchi et al., 2011), and metabolic inhibitors have been shown to block the refilling process (Secchi and Zwieniecki, 2016; Trifilò et al., 2014).

Considering the proposed role of stored *NSC* in the hydraulic recovery process, it has been postulated that vessel-associated parenchyma and/or phloem play key roles in the xylem refilling mechanism (Salleo et al., 2004; Secchi et al., 2017). In fact, the amount of wood parenchyma correlates to the quantity of *NSC* stored in the stem (Morris et al., 2018; Plavcová et al., 2016; Pratt and Jacobsen, 2017) and, hence, with the potential osmotic forces generated in refilling conduits after drought relief (Nardini et al., 2018).

Previous studies have also shown that post-drought hydraulic recovery is often vigorous and complete in species characterized by low wood density and high stem capacitance (Ogasa et al., 2013; Trifilò et al., 2015), while species with denser wood often do not recover at all their xylem functionality upon rehydration. Wood density and capacitance are inversely correlated (Savi et al., 2017) and generally associated with the percentage of wood volume occupied by parenchyma (Pratt et al., 2007; Pratt and Jacobsen, 2017; Scholz et al., 2007; Zheng and Martínez-Cabrera, 2013), suggesting a possible link between parenchyma abundance, *NSC* availability, and species-specific capacity to reverse xylem embolism upon rehydration.

In the present study, we explicitly tested the hypothesis that species-specific recovery from embolism is correlated with parenchyma abundance, as a proxy for the amount of *NSC* available to generate the osmotic forces during the refilling process.

2. Material and methods

Experiments were performed during summer 2017 on twelve adult angiosperm species (Table 1), growing in the campus of University of Messina, Italy (38°15′36″N; 15°35′53″E; 51 m a.s.l.). Species were selected on the basis of a preliminary screening, taking into account the xylem parenchyma fraction (Fig. 1) and the species-specific vulnerability to xylem embolism (see subsection 2.3).

2.1. Measurements of branches anatomical traits

Three branches per species, including those used for hydraulic measurements, were collected from different individuals to estimate the amount of wood parenchyma. For each sample, transverse and tangential micro-sections (25 μm thick) were cut with a rotary microtome (RM 2245, Leica Biosystems, Nussloch, Germany). Sections were stained with a solution of safranin and astra blue (1% and 0.5% in distilled water respectively), and fixed on glass slides with Eukitt (BiOptica, Milano, Italy). Images were acquired at 100× magnification, using a D-sight slide scanner (Menarini Group, Florence, Italy) and analysed with ImageJ version 2.0.0.

The area of axial parenchyma (*AP*), including both apotracheal and paratracheal cells, and of radial parenchyma (*RP*), were measured. For each image, an area of approximately 1 mm^2 was selected and the areas occupied by the parenchyma cells were manually outlined. *AP* and *RP* areas were converted in percentage values by dividing the recorded areas for the corresponding analysed area. Since the axial and radial parenchyma cells orientate perpendicularly to the transverse and tangential section, respectively, the percentage of xylem parenchyma cells in a unit of wood volume (*RAP*) was estimated as: $RAP = AP + RP$. Additional anatomical measurements were performed on branch cross sections using ROXAS v. 3.0.139 (von Arx and Carrer, 2014). Analysis was performed on a wedge of known angle (α) centred at the pith for each image. A first manual editing of the images to outline the contour of the pith and of each ring was carried out. For each outlined sector in the wedge, ROXAS automatically measured the area (*A*), the number of xylem conduits (N_c) and the mean conduit area (*MCA*). Then, traits' data (Y^I) of pith area (A_{pith}), xylem ring area (*RA*), total xylem area (*XA*) and total vessel number were up-scaled to the whole cross section as $Y = Y^I/\alpha \times 360$. Vessel density ($V_d$) has been estimated as: (N_c/XA).

2.2. Measurements of maximum vessel length

In order to avoid possible excision artefacts during hydraulic measurements (Venturas et al., 2017), maximum vessel length (*MVL*) was estimated for each species using an air injection method. At least three branches (more than 1 m long) were collected for each species from different individuals, enclosed in a plastic bag and transported to the laboratory within 10 min. The apical end of the samples was cut and connected to a pressure chamber equipped with a precision pressure test gauge (A4A, Ashcroft Inc., Stratford,CT, USA), while the basal end was immersed in a water-filled tray. A pressure of 60 kPa was applied and the basal portion of the stem was observed with a magnifying lens. Progressive 2 cm cuts were made at the basal end, until a stream of air bubbles emerged from the basal cut section, indicating the presence of at least one vessel cut open at both ends. This length was recorded as an estimate of *MVL* (Table 1).

2.3. Vulnerability to xylem embolism

Species-specific vulnerability to xylem embolism was assessed in terms of the xylem pressure values inducing 50% loss of xylem hydraulic conductivity (P_{50}). P_{50} values were obtained by published data for all species (see references in Table 1), except in *M. alba*. For this species, a vulnerability curve was measured using the bench dehydration technique on samples of similar age and dimensions of that used for estimating the ability to recover from xylem embolism. Summarizing, P_{50} values have been obtained by vulnerability curves performed by the bench dehydration method for all species except for *A. unedo* and *P. latifolia*. For these species, P_{50} values have been obtained by vulnerability curves performed by the air-injection method.

Table 1
Names of species, family, abbreviations (*Abbr*), xylem pressure values inducing ~50% loss of xylem hydraulic conductivity (P_{50}), mean values ± SEM of the maximum vessel length (*MVL*, $n = 3$) and of the percentage of wood parenchyma cells (*RAP*, n = 3).

Species	Family	*Abbr*	P_{50} (MPa)	*MVL* (m)	*RAP* (%)
Arbutus unedo L.	Ericaceae	Au	−3.1 (Martínez-Vilalta et al., 2002)	0.24 ± 0.01	19.2 ± 1.0
Ceratonia siliqua L.	Fabaceae	Cs	−2.6 (Trifilò et al., 2015)	0.36 ± 0.005	25.6 ± 4.0
Cercis siliquastrum L.	Fabaceae	Csq	−1.8 (Nardini et al., 2003)	0.20 ± 0.01	17.4 ± 2.2
Eucalyptus camaldulensis Dehnh	Myrtaceae	Ec	−4.6 (Trifilò et al., 2015)	0.90 ± 0.005	14.8 ± 0.2
Laurus nobilis L.	Lauraceae	Ln	−2.5 (Trifilò et al., 2015)	0.42 ± 0.01	17.1 ± 0.5
Morus alba L.	Moaraceae	Ma	−0.9	0.32 ± 0.01	28.6 ± 1.9
Myrtus communis L.	Myrtaceae	Mc	−3.1 (Trifilò et al., 2015)	0.31 ± 0.02	23.0 ± 1.6
Nerium oleander L.	Apocynaceae	No	−1.5 (Trifilò et al., 2015)	0.30 ± 0.02	14.0 ± 1.3
Olea europaea L.	Oleaceae	Oe	−2.1 (Trifilò et al., 2015)	0.66 ± 0.005	16.8 ± 0.8
Phillyrea latifolia L.	Oleaceae	Phi	−6.5 (Martínez-Vilalta et al., 2002)	0.26 ± 0.03	20.0 ± 1.7
Pistacia lentiscus L.	Anacardacieae	Pl	−4.1 (Trifilò et al., 2015)	0.32 ± 0.03	13.7 ± 1.5
Quercus ilex L.	Fagaceae	Qi	−3.3 (Trifilò et al., 2015)	0.91 ± 0.01	28.0 ± 4.0

2.4. *Estimating dehydration time required to reach 50% loss of hydraulic conductivity*

The target 50% loss of hydraulic conductivity was set for experiments aimed at verifying species-specific ability to recover from xylem embolism upon rehydration (see below). Preliminary experiments were performed to get information about species-specific dehydration time intervals necessary to reach the desired loss of conductivity. Samples longer at least 2 times the species-specific *MVL* were detached from plants, put in large plastic bags and transported to the laboratory within about 5 min.

In the laboratory, branches were exposed to air, and the percentage loss of hydraulic conductivity (*PLC*) was measured on stem samples detached at different time intervals (see below for details on hydraulic measurements) until *PLC* ~ 50% was recorded.

2.5. *Estimating species-specific capacity for embolism recovery*

Branches at least 2 times longer than the species-specific *MVL* were cut in air (Torres-Ruiz et al., 2015), enclosed in a plastic bag and transported to the laboratory where they were bench-dehydrated for the species-specific time required to reach a *PLC* of ~50% (see subsection 2.4). Then, the basal end of samples was put into a water-filled tray, and 10 cm cuts were progressively made under water to progressively relax xylem tension and reconnect the xylem network with water, until obtaining sub-samples shorter than the *MVL* (relaxed samples, *R*). This experimental procedure was aimed at avoiding spurious embolism in terminal shoot samples during dehydration (Wheeler et al., 2013). Xylem tension relaxation was checked in at least two branches per species, collected from different samples, by measuring the water potential of leaves previously wrapped in cling film and aluminium foil (at least 1h before the measurement) to assure equilibration with xylem pressure (Ψ_x). Water potential was measured using a pressure bomb in: a) samples collected when *PLC* ~50% was reached (native samples, *N*); b) samples at the end of the cuttings procedure (relaxed samples, *R*); c) *R* samples maintained with their basal end immersed in water for 10 min after the cutting procedure (R_{10min}); d) *R* samples after 1 h rehydration (R_{1h}). The initial *PLC* was measured in *R* samples (PLC_R), and the eventual hydraulic recovery was measured in R_{1h} samples (PLC_{R1h}). Xylem recover ability was calculated as $\Delta PLC = PLC_R - PLC_{R1h}$.

All hydraulic measurements were performed on 10–15 cm long branch segments, using a hydraulic apparatus. Samples were perfused

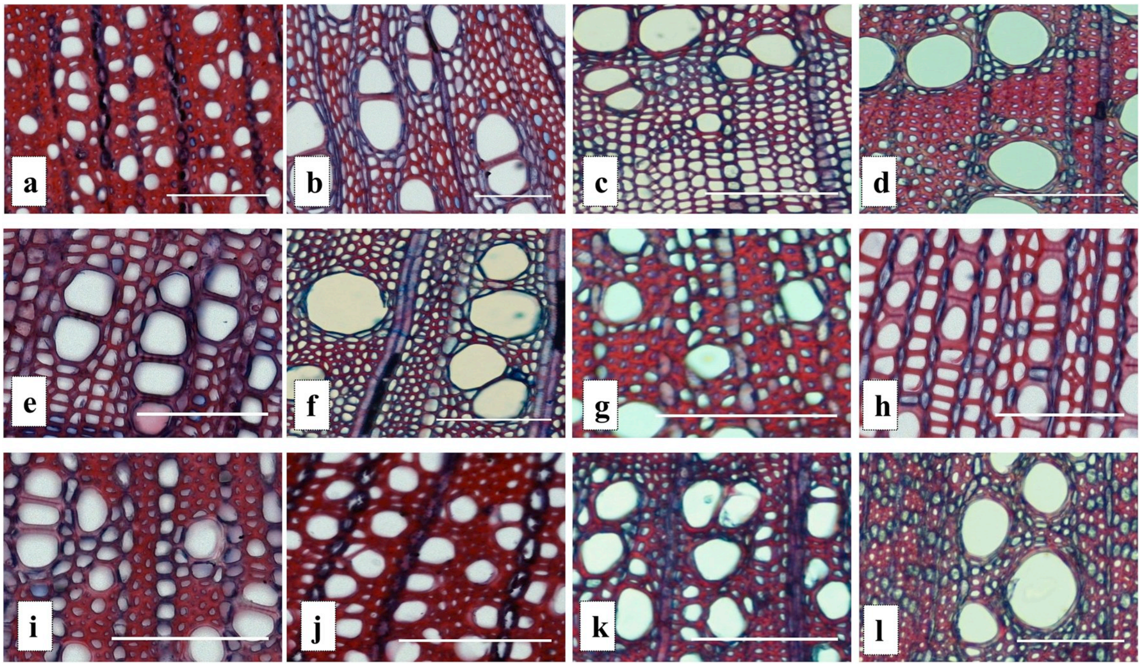

Fig. 1. Images at 100× magnification of transverse sections of: (a) *Arbutus unedo*, (b) *Ceratonia siliqua*, (c) *Cercis siliquastrum*, (d) *Eucalyptus camaldulensis*, (e) *Laurus nobilis*, (f) *Morus alba*, (g) *Myrtus communis*, (h) *Nerium oleander*, (i) *Olea europaea*, (j) *Phillyrea latifolia*, (k) *Pistacia lentiscus*, (l) *Quercus ilex*. Scale bars at 100 μm are shown.

with a solution based on a commercial mineral water containing several ions and with $[K^+]$ adjusted to a value of 15 mM by adding KCl in order to simulate native xylem sap content (Trifilò et al., 2014). The solution was initially perfused at a pressure (P) of 8 kPa and, when the flow (F) became stable, the initial xylem-specific stem hydraulic conductivity (K_s) was calculated as $(F/P) \times (L/A_x)$, where L is the sample length and A_x is the xylem cross sectional area. Samples were then flushed at $P = 0.2$ MPa for 20 min to remove embolism and flow was re-measured at $P = 8$ kPa to obtain K_{max}. The *PLC* was calculated as: $1 - (K_s/K_{max}) \times 100$.

2.6. Impact of phloem girdling on embolism recovery

According to previous studies (Trifilò et al., 2014; Venturas et al., 2015), stem girdling inhibits the embolism repair process. Hence, the effect of girdling on hydraulic recovery was tested in 6 out of 12 species. Branches 2-fold longer than species-specific *MVL* were cut in air, and processed as described in subsection 2.5. However, 1 h before starting the hydraulic measurements, the samples were girdled for their entire length at 15 cm intervals, by removing about 5 mm wide bark rings, avoiding (when possible) areas where leaves were attached. The exposed wood was immediately covered with a thin layer of silicone grease to prevent desiccation (Trifilò et al., 2014). Girdled samples were then measured to estimate their *PLC* at the end of the relaxation procedure and after 1 h rehydration (see subsection 2.5).

2.7. Estimating non-structural carbohydrates

Non-structural carbohydrates (*NSC*) were measured on the same samples used for hydraulic measurements. Just before hydraulic measurements, a 5 cm stem segment was collected from at least 5 samples per treatment, and microwaved at 700 W for 3 min to stop enzymatic activities. Samples were then oven-dried at 70 °C for 24 h and ground to fine powder (particle size < 0.15 mm). Then, 15 ± 1 mg of material were transferred in a 1.5 ml Eppendorf test vial. The super-natant was collected to measure the soluble *NSC* fraction (NSC_{sol}) by means of the anthrone-sulfuric acid assay. A glucose standard curve was used to compare the colorimetric response of the samples, whose absorbance was read at 620 nm, and the *NSC* content was expressed as mg [glucose] g^{-1} [*DW*]. The insoluble fraction was used for starch measurement. Starch digestion was performed overnight at 55 °C, using 100 U of α-Amylase (EC 3.2.1.1, Sigma-Aldrich,St. Louis, MO, USA) and 25 U of Amylogucosidase (EC 3.2.1.3, Sigma-Aldrich, St. Louis, MO, USA) per sample. To prevent further degradation, the samples were boiled for 3 min. For analyses, 2 μl of final supernatant were transferred in a plate reader (1420 Multilabel Counter Victor3, PerkinElmer), with 300 μl final volume of essay buffer (Tris-HCl with $MgCl_2$ 5 mM, $NADP^+$ 125 μM, and MgATP 1 mM) and evaluated by measuring the fluorescence of NADPH (329 and 460 nm for excitation and emission wavelength, respectively). Known amounts of Amylose were also processed and analysed to obtain a calibration curve. The final concentration of starch in the sample was then expressed as mg [starch] g^{-1} [*DW*].

To quantify eventual variations in NSC_{sol} and in starch content during hydraulic recovery following the rehydration procedure, ΔNSC_{sol} and *ΔStarch* were also estimated. In detail, ΔNSC_{sol} was calculated as: $(NSC_{sol,\ R} - NSC_{sol,\ R1h})$ and *ΔStarch* was calculated as: $(Starch_R - Starch_{R1h})$ where $NSC_{sol,\ R}$ and $Starch_R$ were the NSC_{sol} and the starch content, respectively, as recorded in relaxed samples while $NSC_{sol,\ R1h}$ and $Starch_{R1h}$ were the NSC_{sol} and the starch content as recorded in *R* samples after 1h rehydration.

2.8. Statistical analysis

All statistical analyses were performed with the software *R* (v. 3.3.3, R Core Team, 2017). Differences in *PLC* between treatments were tested for each species separately, using Welch's *t*-test (for species with only 2 treatments) and one-way-Welch's ANOVA followed by Games-Howell *post hoc* comparisons (for species with more than 2 treatments) to account for non-homogenous variances. Differences were considered as highly significant for $P < 0.05$, and marginally significant for $P < 0.1$. Spearman's rho (ρ) correlation coefficient among anatomical and hydraulic parameters and *NSC* of all studied species was calculated. For statistically significant correlations ($P < 0.05$), a regression model was calculated.

3. Results

3.1. Vulnerability to xylem embolism and anatomical traits

Across our set of studied species, large variability in vulnerability to xylem embolism estimated in terms of P_{50} was present (from −0.9 MPa in *M. alba* to −6.5 MPa in *P. latifolia*, Table 1). The total amount of wood parenchyma (*RAP*) ranged from about 14% of wood volume in *P. lentiscus* and *N. oleander* to about 29% in *M. alba* (Fig. 1, Table 1). Considerable variation was also observed in terms of maximum vessel length, that ranged between 0.2 m in *C. siliquastrum* to 0.9 m in *E. camaldulensis* and *Q. ilex* (Table 1).

Ray parenchyma (*RP*) was more abundant than axial parenchyma (*AP*) in all the study species (Table S1). Pith area (A_{pith}) ranged widely between species, from about 6% of stem cross-sectional area in *P. lentiscus* and *Q. ilex*, to almost 40% in *C. siliqua* (Table S1, Fig. 3). Large differences were also observed across species in terms of vessel density, V_d (from 73 conduits mm^{-2} in *C. siliqua* to 420 conduits mm^{-2} in *A. unedo* and *P. latifolia*), mean conduit area, *MCA* (from 200 μm^2 in *P. latifolia* to 1400 μm^2 in *M. alba*) and number of conduits, N_c (from 500 in *M. alba* to 3300 in *A. unedo*) (Table S1).

3.2. Embolism recovery in response to rehydration in intact and girdled samples

On the basis of species-specific P_{50} and preliminary experiments, branches of the different species were dehydrated to xylem water potential (Ψ_x) values between about −1 MPa (*C. siliquastrum* and *M. alba*) and −6 MPa (*P. latifolia*) (Table 2), to induce *PLC* values between 40 and 60% (Fig. 2). *PLC* values were measured in samples where xylem tension had been relaxed by progressive cutting samples underwater (Fig. 2, *R* samples). This procedure induced a significant increase in Ψ_x that was already observed at the end of the cutting sequence, when values between −0.4 MPa (*C. siliqua*, *N. oleander* and *Q. ilex*) and −1.1 MPa (*A. unedo* and *O. europaea*) were recorded. After *R* samples had been rehydrated for 10 min (Table 2, R_{10min}), Ψ_x further increased and ranged between −0.2 and −0.45 MPa. After 1 h of rehydration (R_{1h}), Ψ_x was between −0.02 and −0.1 MPa in all the study species (data not shown). The girdling procedure applied to 6 out of 12 species did not affected the pattern of xylem water potential changes. Girdled branches were dehydrated to statistically similar Ψ_x values (Table 2, N_G), and after the fast relaxation procedure (i.e. R_G samples) their Ψ_x was not statistically different from that of non-girdled branches. Similarly, R_G samples had Ψ_x values similar to *R* sample after both 10 min and 1h rehydration.

When branches of different species experiencing *PLC* values of 40–60% (Fig. 2, *R* samples) were rehydrated for 1 h after reconnecting the xylem system to the water source through sequential cuttings based on species-specific *MVL*, different patterns of hydraulic recovery were observed. In seven out of 12 species *PLC* significantly decreased within 1h (Fig. 2, R_{1h}), reaching values between 10 and 20%, while in the remaining five species non-significant or only marginally significant decreases of *PLC* were recorded. It can be noted that, among the four species showing no rise in *PLC* (i.e. embolism reversal), three had *RAP* values < 15% (i.e. *Ec, No, Pl*), while all species showing a significant or a marginally significant *PLC* recovery had *RAP* values > 15% (Table 1).

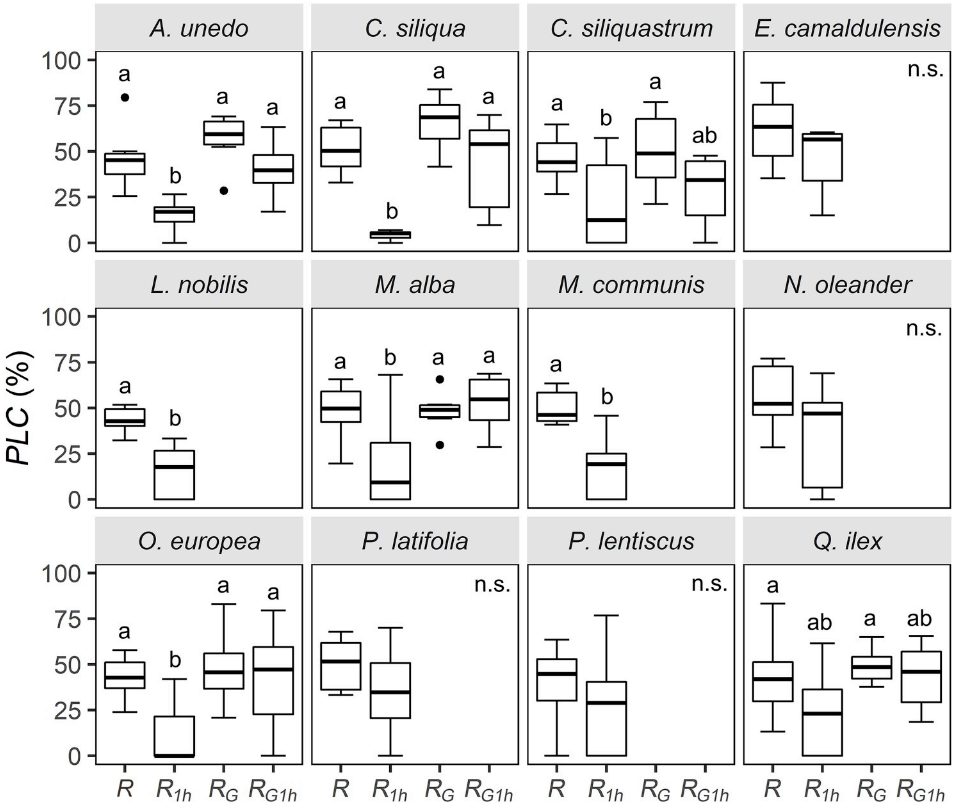

Fig. 2. Mean values ± SEM of the percentage loss of hydraulic conductivity (*PLC*) as recorded in relaxed samples (*R*), *R* samples after 1 h rehydration (R_{1h}), in girdled samples (R_G) and in R_G samples after 1 h rehydration (R_{G1h}). Different letters indicate significant differences from Tukey's pairwise comparisons or *t*-test ($n \geq 6$).

Among the species where a significant hydraulic recovery was observed, six were treated with a girdling procedure. In all these species, removing the bark resulted in the suppression of the *PLC* recovery pattern, that remained close to values recorded in *R* samples even after 1h rehydration (Fig. 2).

3.3. NSC and starch consumption: relationships with the embolism reversal ability

The different studied species also widely differed in terms of starch and soluble carbohydrates (NSC_{sol}). In particular, in *R* samples, starch content ranged between about 3 (*Q. ilex*) and 190 mg g^{-1} (*C. siliqua*), while NSC_{sol} ranged between 50 (*P. latifolia*) and 150 mg g^{-1} (*P. lentiscus*) (Table S2, Fig. 3). Both starch and NSC_{sol} were different between *R* and R_{1h} samples, but because of the large variability of data, these differences turned out to be non-significant. Nonetheless, NSC_{sol} decreased in the species showing a significant decrease of *PLC* following rehydration. In fact, a positive correlation was recorded between the decrease in *PLC* following re-hydration (ΔPLC) and ΔNSC_{sol} (Fig. 3a).

3.4. Correlations between pith area and xylem hydraulic traits

Both P_{50} and ΔPLC were correlated with the percentage pith area, with species showing the largest volume of wood occupied by pith being more vulnerable to xylem embolism and showing the largest *PLC* recovery upon rehydration (Fig. 3b and c).

4. Discussion

Our results show that excised branches of twelve woody species have different capacities to recover from embolism after 1h rehydration, despite similar starting *PLC* levels and similarly high (close to 0) water potential reached at the end of the rehydration period. We show that this species-specific capacity to reverse embolism is correlated with the amount of parenchyma cells, especially of the pith area, and apparently depends on the consumption of soluble *NSC*.

In accordance with previous studies (Trifilò et al., 2014; Venturas et al., 2015), detached branches experiencing substantial embolism level recovered their hydraulic functionality following short-term rehydration. It has been suggested that cut branches put in contact with water can refill xylem conduits via purely physical effects related to capillarity, that would not occur in intact plants (Knipfer et al., 2017). However, it can be noted that capillarity may partially explain the ascent of sap within a vessel. In accordance, it cannot occur in longer and wider vessels. The species-specific occurrence of embolism reversal detected in our experiments, despite similar water potential values reached at the end of the rehydration, calls for a role of biological processes in this phenomenon. In addition, it is unlikely that our *PLC* data were affected to a significant extent by a 'cutting artefact' as described by Wheeler et al. (2013). This is because the samples were processed taking into careful account species-specific maximum vessel length, and were also subjected to a xylem tension relaxation procedure before performing hydraulic measurements. This procedure resulted in xylem water potential values between −0.2 and −0.5 MPa in all the species at the time of cutting, i.e. a range of values recommended by Torres-Ruiz et al. (2015) as optimal for final excision of samples to be used in hydraulic measurements.

The biological nature of the embolism refilling process detected in our experiments is also confirmed by the effects of experimental girdling on the recovery process. In fact, selective removal of the bark from branches resulted in similar patterns of water potential decline and recovery during dehydration and rehydration, and similar *PLC* levels at the end of dehydration. However, girdled samples did not recover the *PLC* values after 1h rehydration, in accordance with previous observations in excised branches (Trifilò et al., 2014; Venturas et al., 2015) or intact plants (Christman et al., 2012). In a recent study, Salmon et al. (2018) have shown that detached branches of *Betula pendula* can refill embolized conduits even under moderate residual negative stem water potential, but the recovery process disappeared when living cells were killed with a heat treatment. Schmitz et al.

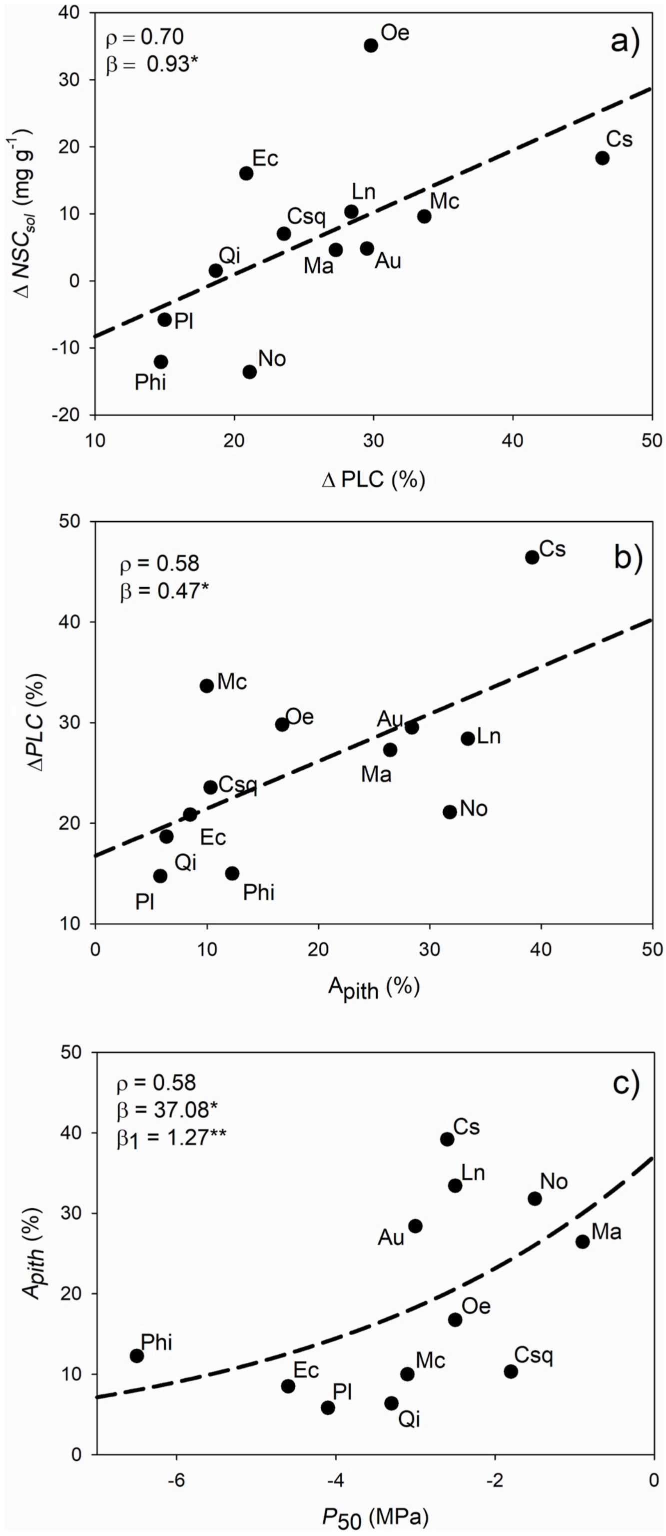

Fig. 3. Relationships between: a) changes in the soluble non-structural carbohydrate content during hydraulic recovery following the rehydration (ΔNSC_{sol}) and the xylem recovery ability (ΔPLC); b) recovery ability (ΔPLC) and pith area (A_{pith}) and c) pith area (A_{pith}) and xylem pressure values inducing 50% loss of xylem hydraulic conductivity (P_{50}). Species abbreviations are reported in Table 1. Regression lines (dotted lines) and related β coefficients values are reported. Significance level: $^{*}P < 0.05$, $^{**}P < 0.01$.

(2012) reported that inhibition of NSC production by bark and wood photosynthesis resulted in the impairment of embolism repair processes in different mangrove species. All these effects would be consistent with the proposed role of bark, phloem and living cells in general as sources of energy, solutes and water necessary to provide the driving forces and the water volumes to refill embolized xylem conduits (Nardini et al., 2018).

Our results suggest that embolism reversal was more effective in species with higher amount of parenchyma cells in their stems, and especially with higher pith area. Taking into account the potential impact of wood parenchyma on wood density, our data are in line with previous studies suggesting that embolism reversal is more likely to be observed in species with lower wood density, which are often those more vulnerable to xylem embolism formation under drought (Nardini et al., 2013; Santini et al., 2016). Although we could not detect a correlation between amount of wood parenchyma and quantity of stored NSC, such a relationship has been previously reported in different assemblages of species (Plavcová et al., 2016; Pratt and Jacobsen, 2017). Moreover, the correlations recorded between the magnitude of PLC recovery and the consumption of soluble NSC and between the ΔPLC and A_{pith} strongly suggest that abundant parenchyma cells might be important in the hydraulic recovery mechanism as a source of carbohydrates, or as a source of water due to the generally high capacitance of woods with high parenchyma fractions (Pratt et al., 2007; Secchi et al., 2017; Trifilò et al., 2015).

Pith cells have been recognized acting as water and carbon storage reservoirs especially in succulent species (Goldstein et al., 1984; Hearn, 2009). Nevertheless, starch grains have been found also in the pith of some deciduous species and in palms (Essiamah and Eschrich, 1985; Pei-Lang et al., 2006; Piispanen and Saranpää, 2001). Therefore, it could be speculated that an abundant percentage of pith cells and RP, contributing to water and/or carbon storage, are both involved in xylem embolism reversal, as our results suggest. This hypothesis, however, needs to be further investigated *in planta*.

The correlation observed across species between ΔPLC recovery and the change in ΔNSC_{sol} recorded during the recovery process is consistent with previous studies suggesting a role for carbohydrates in the embolism reversal process (Savi et al., 2016; Yoshimura et al., 2016; Wang et al., 2018). Progressive depletion of starch and accumulation of soluble sugars in xylem sap has been reported for poplar stems undergoing drought stress (Secchi and Zwieniecki, 2012). It has been suggested that this process primes the xylem for embolism repair via generation of localized osmotic pressures once plant water potential rises again to water potential close to zero following drought relief (Secchi and Zwieniecki, 2016). In our study species, only those undergoing a decline of NSC_{sol} during the rehydration phase finally showed a significant recovery of PLC, supporting the view that during the dehydration phase soluble sugars were released and then used for the refilling process. However, the fate of these sugars after hydraulic recovery is not clear, and our data do not provide evidence for their inter-conversion in starch, or consumption by respiratory metabolism.

The conditions experienced by detached branches dehydrated and rehydrated in the laboratory are obviously different from those of an intact plant. Hence, our results do not necessarily provide evidence that embolism reversal does occur *in planta*. One of the most obvious differences between detached branches and intact plants is related to the conditions during the rehydration phase. In fact, detached branches put in contact with water might eventually rehydrate to water potential values close to zero, a condition that might favor the spontaneous dissolution of the gas phase in embolized conduits (Venturas et al., 2017), or would strongly favor active refilling of conduits avoiding drawdown of refilling water by still functioning conduits under tension. A condition of 'zero water potential' is generally not possible for intact plants, unless stem or root pressure are generated (Gleason et al., 2017). In fact, even when at field capacity, soils have slightly negative water potential due to the presence of solutes, and in any case perfect

Table 2

Mean values ± SD (at least $n = 2$) of the xylem water potential measured in: intact and girdled samples collected when a percentage loss of hydraulic conductivity of about 50% was reached (N and N_G, respectively), intact and girdled samples at the end of the cuttings procedure (R and R_G, respectively) as well as in R and R_G samples maintained with their basal end immersed in water for 10 min after the cutting procedure (R_{10min} and $R_{G,\ 10min}$, respectively). Different letters indicate significant differences for Tukey's pairwise comparisons.

Abbr	N	N_G	R	R_G	R_{10min}	$R_{G,\ 10min}$
Au	−3.90 ± 0.23a	−4.05 ± 0.03a	−1.13 ± 0.21b	−1.07 ± 0.14b	−0.35 ± 0.03c	−0.27 ± 0.02c
Cs	−0.96 ± 0.03a	−1.13 ± 0.17a	−0.45 ± 0.05bc	−0.60 ± 0.17b	−0.20 ± 0.00c	−0.22 ± 0.01c
Csq	−2.30 ± 0.02a	−2.42 ± 0.08a	−0.39 ± 0.16b	−0.40 ± 0.05b	−0.20 ± 0.09b	−0.20 ± 0.01b
Ec	−2.27 ± 0.38a	/	−0.65 ± 0.05b	/	−0.33 ± 0.06b	/
Ln	−2.75 ± 0.15a	/	−0.83 ± 0.07b	/	−0.19 ± 0.09c	/
Ma	−1.05 ± 0.05a	−1.18 ± 0.19a	−0.50 ± 0.00b	−0.50 ± 0.01b	−0.18 ± 0.00b	−0.19 ± 0.00b
Mc	−3.40 ± 0.29a	/	−1.07 ± 0.37b	/	−0.43 ± 0.09b	/
No	−1.08 ± 0.19a	/	−0.42 ± 0.02b	/	−0.25 ± 0.05b	/
Oe	−2.57 ± 0.25a	−2.71 ± 0.11a	−1.10a ± 0.20bc	−1.15 ± 0.25b	−0.45 ± 0.05c	−0.45 ± 0.04c
Phi	< -5.27a	/	−1.34 ± 0.10b	/	−0.43 ± 0.04c	/
Pl	−4.30 ± 0.24a	/	−1.37 ± 0.24b	/	−0.47 ± 0.12c	/
Qi	−3.08 ± 0.12a	−3.35 ± 0.05a	−0.40 ± 0.07b	−0.45 ± 0.05b	−0.25 ± 0.05b	−0.25 ± 0.05b

equilibration of plant water potential with soil water potential is rare (Donovan et al., 2001). As a consequence, most woody plants rehydrated by natural precipitation following a prolonged drought are likely to experience some residual negative pressure in their functioning xylem conduits, possibly making impossible embolism reversal. Previous studies have suggested that embolism reversal is possible even under conditions of residual negative water potential (Nardini et al., 2008; Stiller et al., 2005), and this has been explained by anatomically based hydraulic isolation of refilling conduits from still functioning ones (Ooeda et al., 2017).

In conclusion, while the eventual occurrence of embolism refilling under tension in the study species needs to be further investigated, our data reports experimental results supporting the hypothesis that refilling capacity of branches is species-specific and related to the amount of parenchyma and *NSC*.

Author contributions

AN, PT and VC conceived and designed the experiment. PT, NK, VC and SV performed the measurements. FP performed the statistical analysis. AN and PT wrote the manuscript, with contributions by all Authors. All authors read and approved.

Acknowledgments

We are very grateful to Dipartimento Regionale Azienda Foreste Demaniali, Messina, Sicily, Italy, for kindly providing plant material.

Appendix A. Supplementary data

Supplementary data to this article can be found online at https://doi.org/10.1016/j.plaphy.2019.04.013.

References

Beikircher, B., Mayr, S., 2017. Annual patterns of xylem embolism in high-yield apple cultivars. Funct. Plant Biol. 44, 587–596.

Brodersen, C.R., Knipfer, T., McElrone, A.J., 2018. Vivo visualization of the final stages of xylem vessel refilling in grapevine (*Vitis vinifera*) stems. New Phytol. 217, 117–126.

Brodersen, C.R., McElrone, A.J., 2013. Maintenance of xylem network transport capacity: a review of embolism repair in vascular plants. Front. Plant Sci. 4, 108.

Chitarra, W., Balestrini, R., Vitali, M., Pagliarani, C., Perrone, I., Schubert, A., Lovisolo, C., 2014. Gene expression in vessel-associated cells upon xylem embolism repair in *Vitis vinifera* L. petioles. Planta 239, 887–899.

Choat, B., Brodribb, T.J., Brodersen, C.R., Duursma, R.A., López, R., Medlyn, B.E., 2018. Triggers of tree mortality under drought. Nature 558, 531–539.

Christman, M.A., Sperry, J.S., Smith, D.D., 2012. Rare pits, large vessels and extreme vulnerability to cavitation in a ring-porous tree species. New Phytol. 193, 713–720.

Cochard, H., Delzon, S., 2013. Hydraulic failure and repair are not routine in trees. Ann. For. Sci. 70, 659–661.

Donovan, L.,A., Linton, M.J., Richards, J.H., 2001. Predawn plant water potential does not necessarily equilibrate with soil water potential under well-watered conditions. Oecologia 129, 328–335.

Essiamah, S., Eschrich, W., 1985. Changes of starch content in the storage tissues of deciduous trees during winter and spring. Int. Assoc. Wood Anat. Bull. 6 97-10.

Gleason, S.M., Wiggans, D.R., Bliss, C.A., Young, J.S., Cooper, M., Willi, K.R., Comas, L.H., 2017. Embolized stems recover overnight in *Zea mays*: the role of soil water, root pressure, and nighttime transpiration. Front. Plant Sci. 8, 662.

Goldstein, G., Meinzer, F.C., Monasterio, M., 1984. The role of capacitance in the water balance of Andean giant rosette species. Plant Cell Environ. 2, 397–406.

Hearn, D.J., 2009. Descriptive anatomy and evolutionary patterns of anatomical diversification in *Adenia* (Passifloraceae). Aliso 27, 13–38.

Klein, T., Zeppel, M.J.B., Anderegg, W.R.L., Bloemen, J., De Kauwe, M.G., Hudson, P., Ruehr, N.K., Powell, T.L., von Arx, G., Nardini, A., 2018. Xylem embolism refilling and resilience against drought-induced mortality in woody plants: processes and trade-offs. Ecol. Res. 33, 839–855.

Knipfer, T., Cuneo, I.F., Brodersen, C.R., McElrone, A.J., 2016. In situ visualization of the dynamics in xylem embolism formation and removal in the absence of root pressure: a study on excised grapevine stems. Plant Physiol. 171, 1024–1036.

Knipfer, T., Cuneo, I.F., Earles, M., Reyes, C., Brodersen, C.R., McElrone, A.J., 2017. Storage compartments for capillary water rarely refill in an intact woody plant. Plant Physiol. 175, 1649–1660.

Lesk, C., Rowhani, P., Ramankutty, N., 2016. Influence of extreme weather disasters on global crop production. Nature 529, 84–87.

Love, D.M., Sperry, J.S., 2018. In situ embolism induction reveals vessel refilling in a natural aspen stand. Tree Physiol. 38, 1006–1015.

Martin-StPaul, N., Delzon, S., Cochard, H., 2017. Plant resistance to drought depends on timely stomatal closure. Ecol. Lett. 20, 1437–1447.

Martínez-Vilalta, J., Pinol, J., Beven, K., 2002. A hydraulic model to predict drought-induced mortality in woody plants: an application to climate change in the Mediterranean. Ecol. Model. 155, 127–147.

Martorell, S., Diaz-Espejo, A., Medrano, H., Ball, M.C., Choat, B., 2014. Rapid hydraulic recovery in *Eucalyptus pauciflora* after drought: linkages between stem hydraulics and leaf gas exchange. Plant Cell Environ. 37, 617–626.

Mayr, S., Kartusch, B., Kikuta, S., 2014. Evidence for air-seeding: watching the formation of embolism in conifer xylem. J. Plant Hydraul. 1 e0004.

Morris, H., Plavcová, L., Gorai, M., Klepsch, M.M., Kotowska, M., Schenk, H.J., Jansen, S., 2018. Vessel-associated cells in angiosperm xylem: highly specialized living cells at the symplast–apoplast boundary. Am. J. Bot. 105, 1–10.

Nardini, A., Battistuzzo, M., Savi, T., 2013. Shoot desiccation and hydraulic failure in temperate woody angiosperms during an extreme summer drought. New Phytol. 200, 322–329.

Nardini, A., Lo Gullo, M.A., Salleo, S., 2011. Refilling embolized xylem conduits: is it a matter of phloem unloading? Plant Sci. 180, 604–611.

Nardini, A., Ramani, M., Gortan, E., Salleo, S., 2008. Vein recovery from embolism occurs under negative pressure in leaves of sunflower (*Helianthus annuus*). Physiol. Plantarum 133, 755–764.

Nardini, A., Salleo, S., Raimondo, F., 2003. Changes in leaf hydraulic conductance correlate with leaf vein embolism in *Cercis siliquastrum* L. Trees 17, 529–534.

Nardini, A., Savi, T., Trifilò, P., Lo Gullo, M.A., 2018. Drought stress and the recovery from xylem embolism in woody plants. Prog. Bot. 79, 197–231.

Ooeda, H., Terashima, I., Taneda, H., 2017. Structures of bordered pits potentially contributing to isolation of a refilled vessel from negative xylem pressure in stems of *Morus australis* Poir.: testing of the pit membrane osmosis and pit valve hypotheses. Plant Cell Physiol. 58, 354–364.

Ogasa, M., Miki, N.H., Murakami, Y., Yoshikawa, K., 2013. Recovery performance in xylem hydraulic conductivity is correlated with cavitation resistance for temperate deciduous tree species. Tree Physiol. 33, 335–344.

Peguero-Pina, J.J., Mendoza-Herrer, O., Gil-Pelegrín, E., Sancho-Knapik, D., 2018. Cavitation limits the recovery of gas exchange after severe drought stress in holm oak (*Quercus ilex* L.). Forests 9, 443.

Perrone, I., Pagliarani, C., Lovisolo, C., Chitarra, W., Roman, F., Schubert, A., 2012. Recovery from water stress affects grape leaf petiole transcriptome. Planta 235, 1383–1396.

Pei-Lang, A.T., Mohamed, A.M.D., Karim, A.A., 2006. Sago starch and composition of associated components in palms of different growth stages. Carbohydr. Polym. 63, 283–286.

Piispanen, R., Saranpää, P., 2001. Variation of non-structural carbohydrates in silver birch (*Betula pendula* Roth) wood. Trees (Berl.) 15, 444–451.

Plavcová, L., Hoch, G., Morris, H., Ghiasi, S., Jansen, S., 2016. The amount of parenchyma and living fibers affects storage of nonstructural carbohydrates in young stems and roots of temperate trees. A. J. Bot. 103, 603–612.

Pratt, R.B., Jacobsen, A.L., Ewers, F.W., Davis, S.D., 2007. Relationships among xylem transport, biomechanics and storage in stems and roots of nine Rhamnaceae species of the California chaparral. New Phytol. 174, 787–798.

Pratt, R.B., Jacobsen, A.L., 2017. Conflicting demands on angiosperm xylem: tradeoffs among storage, transport and biomechanics. Plant Cell Environ. 40, 897–913.

Raschke, K., 1976. How stomata resolve the dilemma of opposing priorities. Phil. Trans. Roy. Soc. Lond. B 273, 551–560.

Salleo, S., Lo Gullo, M.A., Trifilò, P., Nardini, A., 2004. New evidence for a role of vessel-associated cells and phloem in the rapid xylem refilling of cavitated stems of *Laurus nobilis* L. Plant Cell Environ. 27, 1065–1076.

Salleo, S., Trifilò, P., Esposito, S., Nardini, A., Lo Gullo, M.A., 2009. Starch-to-sugar conversion in wood parenchyma of field-growing *Laurus nobilis* plants: a component of the signal pathway for embolism repair? Funct. Plant Biol 36, 815–825.

Salmon, Y., Lintunen, A., Lindfors, L., Suhonen, H., Sevanto, S., Vesala, T., Hölttä, T., 2018. Silver birch ability to refill fully embolised xylem conduits under tension. Acta Hortic. (Wagening.). https://doi.org/10.17660/ActaHortic.2018.1222.10.

Santini, N.S., Cleverly, J., Faux, R., Lestrange, C., Rumman, R., Eamus, D., 2016. Xylem traits and water-use efficiency of woody species co-occurring in the Ti Tree Basin arid zone. Trees (Berl.) 30, 295–303.

Savi, T., Casolo, V., Luglio, J., Bertuzzi, S., Trifilò, P., Lo Gullo, M.A., Nardini, A., 2016. Species-specific reversal of stem xylem embolism after a prolonged drought correlates to endpoint concentration of soluble sugars. Plant Physiol. Biochem. 106, 198–207.

Savi, T., Love, V.L., Dal Borgo, A., Martellos, S., Nardini, A., 2017. Morpho-anatomical and physiological traits in saplings of drought-tolerant Mediterranean woody species. Trees (Berl.) 31, 1137–1148.

Schmitz, N., Egerton, J.J.G., Lovelock, C.E., Ball, M.C., 2012. Light-dependent maintenance of hydraulic function in mangrove branches: do xylary chloroplasts play a role in embolism repair? New Phytol. 195, 40–46.

Scholz, F.G., Bucci, S.J., Goldstein, G., Meinzer, F.C., Franco, A.C., Miralles-Wilhelm, F., 2007. Biophysical properties and functional significance of stem water storage tissues in Neotropical savanna trees. Plant Cell Environ. 30, 236–248.

Schuster, A.C., Burghardt, M., Riederer, M., 2017. The ecophysiology of leaf cuticular transpiration: are cuticular water permeabilities adapted to ecological conditions? J. Exp. Bot. 68, 5271–5279.

Secchi, F., Gilbert, M.E., Zwieniecki, M.A., 2011. Transcriptome response to embolism formation in stems of *Populus trichocarpa* provides insight into signaling and the biology of refilling. Plant Physiol. 157, 1419–1429.

Secchi, F., Pagliarani, C., Zwieniecki, M.A., 2017. The functional role of xylem parenchyma cells and aquaporins during recovery from severe water stress. Plant Cell Environ. 40, 858–871.

Secchi, F., Zwieniecki, M.A., 2011. Sensing embolism in xylem vessels: the role of sucrose as a trigger for refilling. Plant Cell Environ. 34, 514–524.

Secchi, F., Zwieniecki, M.A., 2012. Analysis of xylem sap from functional (nonembolized) and nonfunctional (embolized) vessels of *Populus nigra*: chemistry of refilling. Plant Physiol. 160, 955–964.

Secchi, F., Zwieniecki, M.A., 2016. Accumulation of sugars in the xylem apoplast observed under water stress conditions is controlled by xylem pH. Plant Cell Environ. 39, 2350–2360.

Stiller, V., Sperry, J.S., Lafitte, R., 2005. Embolized conduits of rice (*Oryza sativa*, Poaceae) refill despite negative xylem pressure. A. J. Bot. 92, 1970–1974.

Tomasella, M., Häberle, K.H., Nardini, A., Hesse, B., Machlet, S., Matyssek, R., 2017. Post-drought hydraulic recovery is accompanied by non-structural carbohydrate depletion in the stem wood of Norway spruce saplings. Sci. Rep. 7, 14308.

Tomasella, M., Nardini, A., Hesse, B., Machlet, A., Matyssek, R., Häberle, K.H., 2019. Close to the edge: effects of repeated severe drought on stem hydraulics and non-structural carbohydrates in European beech saplings. Tree Physiol. https://doi.org/10.1093/treephys/tpy142.

Torres-Ruiz, J.M., Jansen, S., Choat, B., McElrone, A.J., Cochard, H., Brodribb, T.J., Badel, E., Burlett, R., Bouche, P.S., Brodersen, C.R., Li, S., Morris, H., Delzon, S., 2015. Direct X-Ray microtomography observation confirms the induction of embolism upon xylem cutting under tension. Plant Physiol. 167, 40–43.

Trifilò, P., Casolo, V., Raimondo, F., Petrussa, E., Boscutti, F., Lo Gullo, M.A., Nardini, A., 2017. Effects of prolonged drought on stem non-structural carbohydrates content and post-drought hydraulic recovery in *Laurus nobilis* L.: the possible link between carbon starvation and hydraulic failure. Plant Physiol. Biochem. 120, 232–241.

Trifilò, P., Nardini, A., Lo Gullo, M.A., Barbera, P.M., Savi, T., Raimondo, F., 2015. Diurnal changes in embolism rate in nine dry forest trees: relationships with species-specific xylem vulnerability, hydraulic strategy and wood traits. Tree Physiol. 35, 694–705.

Trifilò, P., Raimondo, F., Lo Gullo, M.A., Barbera, P.M., Salleo, S., Nardini, A., 2014. Relax and refill: xylem rehydration prior to hydraulic measurements favours embolism repair in stems and generates artificially low PLC values. Plant Cell Environ. 37, 2491–2499.

Tyree, M.T., Sperry, J.S., 1989. Vulnerability of xylem to cavitation and embolism. Ann. Rev. Plant Phys. Mol. Bio. 40, 19–38.

Tyree, M.T., Vargas, G., Engelbrecht, B.M.J., Kursar, T.A., 2002. Drought until death do us part: a case study of the desiccation-tolerance of a tropical moist forest seedling-tree, *Licania platypus* (Hemsl.) Fritsch. J. Exp. Bot. 53, 2239–2247.

Urli, M., Porté, A.J., Cochard, H., Guengant, Y., Burlett, R., Delzon, S., 2013. Xylem embolism threshold for catastrophic hydraulic failure in angiosperm trees. Tree Physiol. 33, 672–683.

Venturas, M.D., MacKinnon, E.D., Jacobsen, A.L., Pratt, R.B., 2015. Excising stem samples underwater at native tension does not induce xylem cavitation. Plant Cell Environ. 38, 1060–1068.

Venturas, M.D., Sperry, J.S., Hacke, U.G., 2017. Plant xylem hydraulics: what we understand, current research, and future challenges. J. Integr. Plant Biol. 59, 356–389.

von Arx, G., Carrer, M., 2014. ROXAS – a new tool to build centuries-long tracheid-lumen chronologies in conifers. Dendrochronologia 32, 290–293.

Wang, A.Y., Han, S.J., Zhang, J.H., Wang, M., Yin, X.H., Fang, L.D., Yang, D., Hao, G.Y., 2018. The interaction between nonstructural carbohydrate reserves and xylem hydraulics in Korean pine trees across an altitudinal gradient. Tree Physiol. 38, 1792–1804.

Wheeler, J.K., Huggett, B.A., Tofte, A.N., Rockwell, F.E., Holbrook, N.M., 2013. Cutting xylem under tension or supersaturated with gas can generate PLC and the appearance of rapid recovery from embolism. Plant Cell Environ. 36, 1938–1949.

Yoshimura, K., Saiki, S.T., Yazaki, K., Ogasa, M.Y., Shirai, M., Nakano, T., Yoshimura, J., Ishida, A., 2016. The dynamics of carbon stored in xylem sapwood to drought-induced hydraulic stress in mature trees. Sci. Rep. 6, 24513.

Zhang, T., Cao, Y., Chen, Y., Liu, G., 2015. Non-structural carbohydrate dynamics in *Robinia pseudoacacia* saplings under three levels of continuous drought stress. Trees (Berl.) 29, 1837–1849.

Zhang, Y., Xu, J., Su, W., Zhao, X., Xu, X., 2019. Spring precipitation effects on formation of first row of earlywood vessels in *Quercus variabilis* at Qinling Mountain (China). Trees (Berl.). https://doi.org/10.1007/s00468-018-1792-y.

Zheng, J., Martínez-Cabrera, H.I., 2013. Wood anatomical correlates with theoretical conductivity and wood density across China: evolutionary evidence of the functional differentiation of axial and radial parenchyma. Ann. Bot. 112, 927–935.